FERMILAB-PUB-16-043-AE

First Search for a Dark Matter Annual Modulation Signal with NaI(Tl) in the Southern Hemisphere by DM-Ice17

E. Barbosa de Souza,[1] J. Cherwinka,[2] A. Cole,[3,4] A. C. Ezeribe,[3] D. Grant,[5] F. Halzen,[6] K. M. Heeger,[1] L. Hsu,[7] A. J. F. Hubbard,[1,6,*] J. H. Jo,[1] A. Karle,[6] M. Kauer,[1,6] V. A. Kudryavtsev,[3] K. E. Lim,[1] C. Macdonald,[3] R. H. Maruyama,[1,†] F. Mouton,[3] S. M. Paling,[4] W. Pettus,[1,6] Z. P. Pierpoint,[1,6,‡] B. N. Reilly,[1,6,§] M. Robinson,[3] F. R. Rogers,[1] P. Sandstrom,[6] A. Scarff,[3] N. J. C. Spooner,[3] S. Telfer,[3] and L. Yang[8]

(The DM-Ice Collaboration)

[1] *Department of Physics, Yale University, New Haven, Connecticut 06520, USA*
[2] *Physical Sciences Laboratory, University of Wisconsin-Madison, Stoughton, Wisconsin 53589, USA*
[3] *Department of Physics and Astronomy, University of Sheffield, Sheffield S10 2TN, United Kingdom*
[4] *STFC Boulby Underground Science Facility, Boulby Mine, Cleveland TS13 4UZ, United Kingdom*
[5] *Department of Physics, University of Alberta, Edmonton, Alberta T6G 2E1, Canada*
[6] *Department of Physics and Wisconsin IceCube Particle Astrophysics Center, University of Wisconsin-Madison, Madison, Wisconsin 53706, USA*
[7] *Fermi National Accelerator Laboratory, Batavia, Illinois 60510, USA*
[8] *Department of Physics, University of Illinois at Urbana-Champaign, Urbana, Illinois 61801, USA*

(Dated: February 24, 2016)

The first search for a dark matter annual modulation signal with NaI(Tl) target material in the Southern Hemisphere conducted with the DM-Ice17 experiment is presented. DM-Ice17 consists of 17 kg of NaI(Tl) scintillating crystal under 2200 m.w.e. overburden of Antarctic glacial ice. The analysis presented here utilizes a 60.8 kg·yr exposure. While unable to exclude the signal reported by DAMA/LIBRA, the DM-Ice17 data are consistent with no modulation in the energy range of 4-20 keV, providing the strongest limits on WIMP candidates from a direct detection experiment located in the Southern Hemisphere. Additionally, the successful deployment and stable operation of 17 kg of NaI(Tl) crystal over 3.6 years establishes the South Pole ice as a viable location for future underground, low-background experiments.

PACS numbers: 95.35.+d, 29.40.Mc, 95.55.Vj
Keywords: DM-Ice, dark matter, sodium iodide, WIMP, direct detection, annual modulation, South Pole

arXiv:1602.05939v2 [physics.ins-det] 23 Feb 2016

Cosmic observations indicate that the majority of the mass in the universe is not accounted for by the Standard Model of particle physics [1]. Theoretical models favor the weakly interacting massive particle (WIMP) as an explanation for this dark matter. The WIMP dark matter model implies the existence of at least one additional particle with a mass on the GeV to TeV scale and interaction cross section with normal matter on the nano- to zeptobarn scale [2, 3]. The Milky Way is modeled to be surrounded by a halo of dark matter, providing a continuous flux of dark matter through terrestrial detectors [4, 5].

In the standard (WIMP) halo model, the motion of the solar system through the galaxy produces a net velocity relative to the dark matter halo. As the Earth orbits the Sun, the magnitude of the Earth's velocity parallel to the solar velocity changes. As a result, the apparent velocity of the dark matter wind on Earth modulates with a one year period, leading in turn to an annual modulation in the rate of dark matter interactions [5, 6].

A suite of experiments attempting to directly detect WIMP dark matter is underway using a variety of detector technologies [7]. The DAMA/NaI and DAMA/LIBRA experiments have reported observations of an annual modulation signature in thallium-doped sodium iodide (NaI(Tl)) crystals commensurate with WIMP dark matter, with the cumulative signature reaching 9.3σ C.L. [8, 9]. Under the standard dark matter halo model, the constraints for many of the WIMP and WIMP-like models set by other experiments are inconsistent with DAMA's claim for discovery [10–21]. Many alternate explanations for the modulation have been proposed [22–27], but to date, none have been able to fully explain the DAMA signal [28–35].

The DM-Ice experiment aims to resolve this tension by performing an unambiguous test of the DAMA signal using the same target medium and analysis strategy [36]. A positive result would be subject to the same questions of seasonal effects directed at DAMA. Performing the experiment in the Southern Hemisphere, however, inverts the phase of seasonal effects without affecting a dark matter signal. For this reason, the DM-Ice collaboration is working towards a Southern Hemisphere deployment of a large NaI(Tl) array.

DM-Ice17, the first stage of the DM-Ice experimental program, was deployed at the geographic South Pole in December 2010 [37]. Two 8.47 kg crystals originally used in the NAIAD dark matter experiment at the Boulby Underground Laboratory [38] were placed at the bottom of the IceCube detector array [39], with 2457 m (2200 m.w.e.) overburden from the Antarctic ice. This constitutes the first search for annual modulation dark

Operated by Fermi Research Alliance, LLC under Contract No. De-AC02-07CH11359 with the United States Department of Energy

matter signal with NaI(Tl) detectors in the Southern Hemisphere. Only the Sierra Grande germanium experiment has previously performed a direct detection dark matter search in the Southern Hemisphere [40]. As the first search at the South Pole, the primary goal of DM-Ice17 was to verify the feasibility of performing a direct detection dark matter search at the site by assessing the quality and stability of the environment [37]. Here we present the results from an annual modulation search in 3.6 years of data.

The analysis presented here covers the primary physics run of DM-Ice17 from June 16, 2011 to January 28, 2015. With $>99\%$ uptime, this corresponds to a total exposure of 60.8 kg·yr. Each DM-Ice17 crystal is optically coupled to two photomultiplier tubes (PMTs) which detect the scintillation photons. These two assemblies are referred to as Det-1 and Det-2, respectively. Coincidence between paired PMTs provides an online dark noise reduction. For the low energy dark matter analysis, data are recorded into $\sim$600 ns waveforms. Detector details, including the trigger conditions, DAQ configuration, and energy calibration, are described in [37].

Energy information is obtained by integrating the charge over the entire readout. Calibration is performed *in situ* by performing a linear regression between fitted internal gamma peak mean charge and the corresponding simulated peak energies [37]. In this paper, all energies are presented in electron-equivalent energies and referred to as keV for simplicity. The crystal response to gamma rays is linear in two distinct regions ($0-100$ keV and $500-3000$ keV), consistent with previous observations [41, 42]. We observe that the total collected charge associated with a given decay is decreasing over time by $\sim$0.5% per year; the cause of this is not well understood. The calibration includes a time dependence to account for this apparent gain shift.

Running conditions are monitored by sensors on the DAQ mainboards, and their stability is described in [37]. In addition to the monitoring data and normal physics runs, periodic runs without the PMT coincidence requirement and runs without the trigger threshold are taken for detector characterization, particularly characterization of the SPE response. Apart from the aforementioned gain shift and a 0.3°C cooling of the detector as the drill ice column thermalizes with the surrounding ice [43], all detector behaviors (trigger threshold, DAQ deadtime, etc.) exhibit no time-dependence.

The spectrum in the region of interest (ROI) includes a 3 keV peak from ^{40}K contamination in the crystals, an $\sim$15 keV feature from surface ^{238}U contamination, an approximately flat continuum from $0-20$ keV at $3-4$ counts/day/keV/kg (see Fig. 1) from other contaminants in the detector components. The simulation of DM-Ice17 [37] predicts the general shape of these major features, though a number of additional cosmogenically activated components are expected to play a role. To

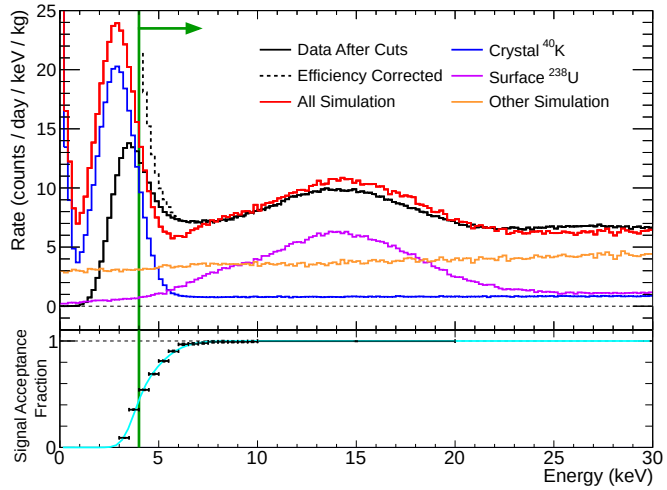

FIG. 1. Energy spectrum of DM-Ice17 from $0-30$ keV(top) and signal acceptance fraction (bottom). Shown are the spectrum from Det-1 after noise cuts (solid black) and with the addition of a cut efficiency correction (dashed black). The full simulation (red) is also shown, along with the contributions from ^{40}K in the crystal (blue), ^{238}U surface contamination on the copper encapsulation of the crystals (violet), and the sum total of backgrounds from other sources (orange). The signal acceptance fraction for the noise cuts is shown below the spectra, with the cut efficiency data (black dots) fit with a functional form (cyan) used in calculations. The green line indicates the 4 keV analysis threshold. Det-2 data are similar, though the lower gain leads to less efficient noise cuts.

enforce stable noise cuts, an analysis threshold of 4 keV for Det-1 and 6 keV for Det-2 is imposed.

Events that are inconsistent with scintillation in NaI(Tl) are rejected in the analysis as noise. Three types of noise trigger the detector: electromagnetic interference (EMI) with the detector monitoring queries, coincident single photoelectrons (SPE), and "thin peaks" which exhibit a decay time an order of magnitude quicker than scintillation and frequently asymmetric pulse heights in the two PMTs [37]. SPE events come about from accidental coincidence of PMT dark noise and phosphorescence from crystal interactions [35], among other sources. Thin peaks are suspected to originate from interactions in the quartz light guides or PMT windows [44, 45]. Thin peaks are the dominant noise source above the analysis threshold for this analysis.

Scintillation in NaI(Tl) has a $\sim$250 ns decay constant associated with photon emission, and photoelectrons arrive at discrete times over the entire readout. EMI events include no photoelectrons, and SPE events include just one photoelectron per PMT. Only thin pulse noise events include multiple photoelectrons; however, all of these photoelectrons are observed as arriving at the same time. Therefore, events with photoelectrons arriving at multiple distinct times are distinguishable as scintilla-

tion. By requiring events to have four photopeaks in each PMT (peak finding cut), $70.8 \pm 0.3\%$ of scintillation events from $4-6$ keV are accepted while producing a signal-to-noise ratio of 230 ± 20.

Peak finding cut efficiency is assessed via analysis of a secondary pulse shape discrimination parameter (pulse integral / pulse height). This parameter provides sufficiently independent discrimination capability between distinct populations that fitting the distribution before and after the peak finding cut enables determination of the peak finding cut efficiency in individual energy bins. The peak finding cut provides information for both Det-1 and Det-2 down to 2 keV; however, the efficiency and stability of the cut have only been directly measured to 4 keV in Det-1 and to 6 keV in Det-2. The behavior of this cut is consistent over time at all energies.

The ROI is split into four separate energy bins ($4-6$, $6-8$, $8-10$, and $10-20$ keV), though the 6 keV analysis threshold of Det-2 precludes analysis of the lowest energy bin. There are, therefore, seven total analysis energy bins between the two crystals, and the physics run is additionally split into half-month time intervals. After correcting for livetime and cut efficiency, the event rates in each energy bin decrease during the physics run by 8%, 9%, 8%, and 6% in the Det-1 event rates for the $4-6$, $6-8$, $8-10$, and $10-20$ keV bins respectively. For Det-2, the decrease is 8%, 8%, and 6% for the $6-8$, $8-10$, and $10-20$ keV bins.

Cosmogenically activated isotopes (such as ^{60}Co and ^{125}I) and the broken ^{232}Th- and ^{238}U-chains produce known changes in the event rate over time [37, 46, 47], though not enough to explain the decrease at the ROI energies. Muon rates are also known to exhibit an approximately sinusoidal time dependence; however, studies of muons and muon-induced phosphorescence in DM-Ice17 have shown no statistically significant muon correlated event rate in the region of interest [35].

Cosmogenically activated ^{3}H provides a possible source of this decrease and is already included in the ANAIS model of NaI(Tl) crystal backgrounds [48]. The ^{238}U surface contamination built into the DM-Ice17 background model [37] includes uncertainties which may also lead to an explanation of the rate decrease. Both ^{3}H and ^{238}U contaminations would exhibit behavior indistinguishable from a linear decrease over the 3.6 year DM-Ice17 physics run. The data are consistent with this behavior.

This analysis accounts for the decrease in rate by incorporating a linear background component into the fit model. Fig. 2 shows the Det-1 event rates for each energy bin after subtracting off the fitted linear component. To perform the modulation analysis, a likelihood minimization fits the event rate over time for each energy bin with a cosinusoid atop the linear background. By varying the number of free parameters, a variety of models can be discussed. For the $4-6$ keV bin of Det-1, chi-squared analysis produces χ^2/d.o.f. $= 86.11 / 87$ for the

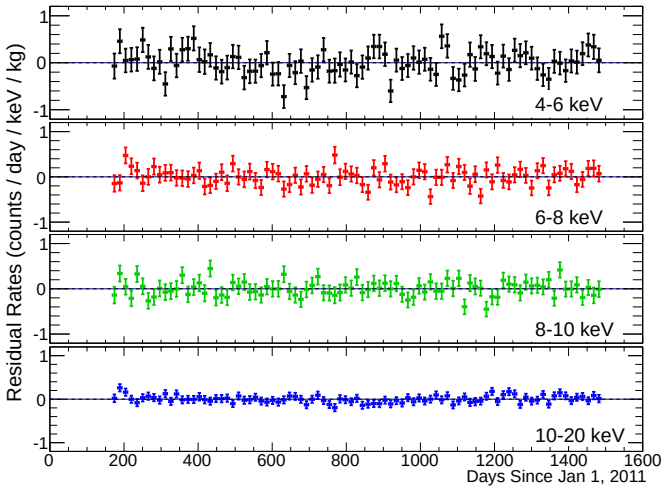

FIG. 2. Residual event rate vs. time for Det-1 after subtracting off the linear rate component. Rates are provided in half month intervals for $4-6$ keV (black), $6-8$ keV (red), $8-10$ keV (green), and $10-20$ keV (blue). The horizontal error bars represent the half-month bin width and the vertical error bars represent $\pm 1\sigma$ error due to statistical and uptime uncertainties. In each of these energy bins, the data are consistent with the null hypothesis. Det-2 data are similarly consistent with no modulation and exhibit a comparable linear rate component.

null hypothesis, χ^2/d.o.f. $= 86.03 / 86$ for an annual modulation (fixed one year period) with the expected dark matter phase (fixed June 2 maximum), and χ^2/d.o.f. $= 84.35 / 85$ for an annual modulation (fixed one year period) with floating phase. The other energy bins are similarly consistent with the null hypothesis, providing no evidence for an annual modulation.

Fixing the period to one year, the best fit to the Det-1 $4-6$ keV bin has a modulation amplitude of 0.05 ± 0.03 counts/day/keV/kg and a maximum on March 16$^{\text{th}} \pm 42$ days. DAMA has not published a floating phase best-fit for $4-6$ keV, so a direct comparison is not possible; however, across $2-6$ keV, DAMA/LIBRA observes a modulation amplitude of 0.011 ± 0.001 and a best fit phase of May 24$^{\text{th}} \pm 7$ days [9]. Log-likelihood analysis comparing annual modulations of each amplitude and phase to the best fit shows that the data from DM-Ice17 are consistent with the null hypothesis (see Fig. 3). The limitations of this detector are also apparent as the DAMA/LIBRA 99% C.L. contour is indistinguishable from the null hypothesis at the 68% C.L.

Modulation fits with fixed period (one year) and phase (152.5 days) are consistent with zero amplitude (see Fig. 4). Comparison of the best fit dark matter-like modulation amplitudes indicates that no significant statement about the DAMA modulation is possible with this dataset.

Under the assumptions of the standard halo model,

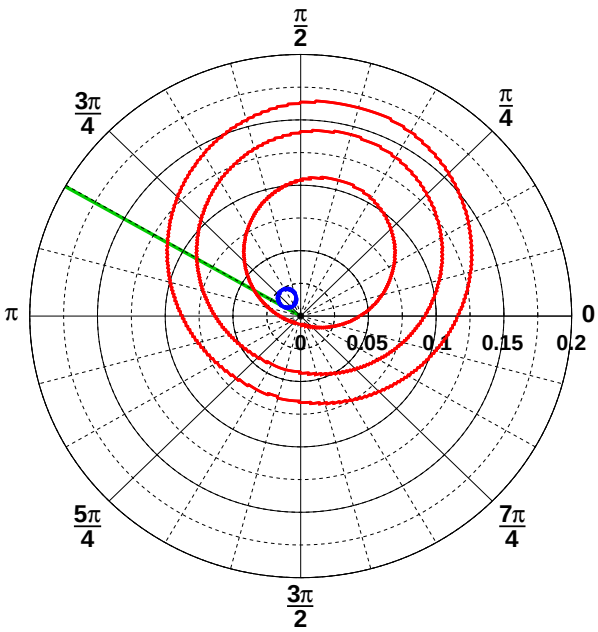

FIG. 3. Allowed regions in amplitude (counts/day/keV/kg) vs. phase for annual modulation fits to the Det-1 4–6 keV data, with contours at (inner to outer) 68%, 95%, and 99% C.L (red). The DAMA/LIBRA 2–4 keV 99% C.L. (blue) is also shown for comparison. Phase of 0 corresponds to January 1st. The predicted phase of a dark matter modulation signal under generic halo models (June 2nd) is indicated by the green line.

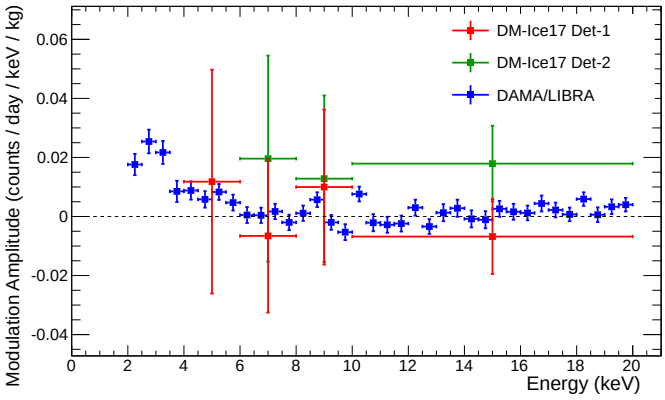

FIG. 4. Amplitude of modulation vs. energy showing maximum likelihood fits for DAMA [9] (blue) and DM-Ice17 rates (Det-1 (red) and Det-2 (green)). The linear background underlying the event rate and the modulation amplitude are free parameters in these fits, with period and phase forced to that of an expected dark matter signal (1 year and 152.5 days, respectively). Horizontal error bars represent the width of the energy bins used for the analysis. Vertical error bars are $\pm 1\sigma$ error on the binned modulation fit amplitudes.

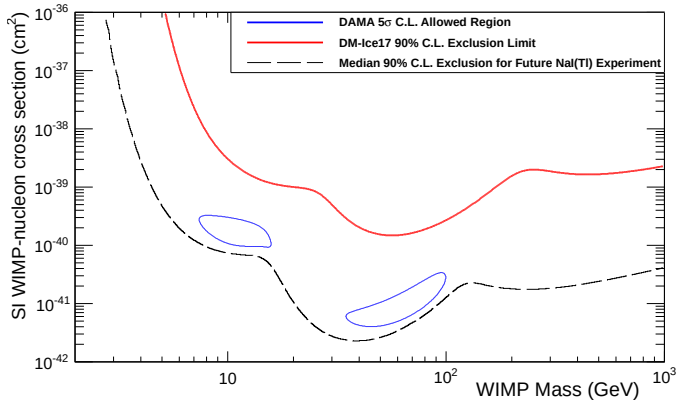

FIG. 5. WIMP exclusion limits at 90% C.L. from the 60.8 kg·yr DM-Ice17 physics dataset (red), with DAMA preferred 5σ C.L. contour (blue) for comparison. As a reference, the projected sensitivity (median 90% C.L.) for a future NaI(Tl)-based detector with 2 counts/day/keV/kg backgrounds in the ROI after 500 kg·yr and a 2 keV analysis threshold is shown in the dashed black line [49].

the information across the entire ROI can be combined to set limits in the WIMP phase space. An exclusion limit (see Fig. 5) is produced via a log-likelihood analysis of the observed binned modulation amplitudes, with predicted modulation amplitudes for particular WIMP candidates as described in [10]. Best fit contours for the full DAMA/LIBRA-phase1 run [9] were produced along with the DM-Ice17 exclusion limit for comparison, based on the methodology from [11]. This assumes a standard halo model with WIMP density of 0.3 GeV/c^2, disk rotation speed of 220 km/s, Earth orbital speed of 29.8 km/s, and galactic escape velocity of 650 km/s. Uncertainties in WIMP-nucleon coupling to different targets do not play a role in the comparison, since DM-Ice17 and DAMA share the NaI(Tl) target material. This constitutes the strongest limit set in the Southern Hemisphere by a direct detection dark matter search, an important step towards an unambiguous statement about the nature of the DAMA signal. A future experiment with 2 counts/day/keV/kg backgrounds in the ROI, a 500 kg·yr exposure, and a 2 keV analysis threshold can definitively test DAMA, as shown in Fig. 5.

The DAMA contours shown here are produced via a log-likelihood analysis rather than via the goodness-of-fit method as described in [11]. We find that while generally similar, the goodness-of-fit methodology introduces an undesirable dependence on the energy binning not present in the log-likelihood method. Given the difference between energy binning of the DM-Ice17 and DAMA data, we perform a log-likelihood analysis on each dataset to avoid introducing effects of this sort.

In summary, we have carried out the first search for a dark matter induced annual modulation with NaI(Tl) as

the target in the Southern Hemisphere. The stable operation of DM-Ice17 over 3.6 years proves the feasibility of the South Pole as a site for future underground, low-background experiments. We find no evidence of annual modulation in the DM-Ice17 dataset from 4 – 20 keV. Although not yet sensitive enough to confirm or exclude DAMA, this constitutes the strongest limit from a direct detection Southern Hemisphere dark matter search to date.

We thank Chris Toth and Emma Meehan for operational support at Boulby Underground Lab. We thank the Wisconsin IceCube Particle Astrophysics Center (WIPAC) and the IceCube collaboration for their on-going experimental support and data management. This work was supported in part by the Alfred P. Sloan Foundation Fellowship, NSF Grants No. PLR-1046816, PHY-1151795, and PHY-1457995, WIPAC, the Wisconsin Alumni Research Foundation, Yale University, the Natural Sciences and Engineering Research Council of Canada, and Fermilab, operated by Fermi Research Alliance, LLC under Contract No. DE-AC02-07CH11359 with the United States Department of Energy. W. P. and A. H. were supported by the DOE/NNSA Stewardship Science Graduate Fellowship (Grant No. DE-FC52-08NA28752) and NSF Graduate Research Fellowship (Grant No. DGE-1256259) respectively.

* Present Address: Department of Physics and Astronomy, Northwestern University, Evanston, Illinois 60208, USA
† Corresponding author: reina.maruyama@yale.edu
‡ Corresponding author: zachary.pierpoint@yale.edu
§ Present Adress: Department of Physics and Astronomy, University of Wisconsin-Fox Valley, Menasha, Wisconsin 54952, USA

[1] P. A. R. Ade *et al.* (Planck), Astron. Astrophys., **571**, A16 (2014), arXiv:1303.5076 [astro-ph.CO].
[2] G. Steigman and M. S. Turner, Nucl. Phys. B, **253**, 375 (1985).
[3] G. Bertone, D. Hooper, and J. Silk, Phys. Rep., **405**, 279 (2005), arXiv:hep-ph/0404175 [hep-ph].
[4] M. W. Goodman and E. Witten, Phys. Rev. D, **31**, 3059 (1985).
[5] A. K. Drukier, K. Freese, and D. N. Spergel, Phys. Rev. D, **33**, 3495 (1986).
[6] K. Freese, J. A. Frieman, and A. Gould, Phys. Rev. D, **37**, 3388 (1988).
[7] P. Cushman *et al.*, in *Community Summer Study 2013: Snowmass on the Mississippi (CSS2013) Minneapolis, MN, USA, July 29-August 6, 2013* (2013) arXiv:1310.8327 [hep-ex].
[8] R. Bernabei *et al.* (DAMA), Int. J. Mod. Phys. D, **13**, 2127 (2004), arXiv:astro-ph/0501412 [astro-ph].
[9] R. Bernabei *et al.* (DAMA), Eur. Phys. J. C, **73**, 2648 (2013), arXiv:1308.5109 [astro-ph.GA].
[10] K. Freese, M. Lisanti, and C. Savage, Rev. Mod. Phys., **85**, 1561 (2013).
[11] C. Savage, G. Gelmini, P. Gondolo, and K. Freese, J. Cosmol. Astropart. Phys., **2009**, 010 (2009).
[12] D. Akerib *et al.* (LUX), (2015), arXiv:1512.03506 [astro-ph.CO].
[13] D. Akerib *et al.* (LUX), (2016), arXiv:1602.03489 [hep-ex].
[14] E. Aprile *et al.* (XENON100), Phys. Rev. Lett., **109**, 181301 (2012), arXiv:1207.5988 [astro-ph.CO].
[15] R. Agnese *et al.* (SuperCDMS), Phys. Rev. Lett., **112**, 241302 (2014), arXiv:1402.7137 [hep-ex].
[16] G. Angloher *et al.* (CRESST-II), Eur. Phys. J. C, **74**, 3184 (2014), arXiv:1407.3146 [astro-ph.CO].
[17] X. Xiao *et al.* (PandaX), Phys. Rev. D, **92**, 052004 (2015), arXiv:1505.00771 [hep-ex].
[18] C. Amole *et al.* (PICO), (2016), arXiv:1601.03729 [astro-ph.CO].
[19] C. Amole *et al.* (PICO), (2015), arXiv:1510.07754 [hep-ex].
[20] M. Felizardo *et al.* (SIMPLE), Phys. Rev. D, **89**, 072013 (2014), arXiv:1404.4309 [hep-ph].
[21] S. C. Kim *et al.*, Phys. Rev. Lett., **108**, 181301 (2012), arXiv:1204.2646 [astro-ph.CO].
[22] J. P. Ralston, (2010), arXiv:1006.5255 [hep-ph].
[23] K. Blum, (2011), arXiv:1110.0857 [astro-ph.HE].
[24] J. H. Davis, Phys. Rev. Lett., **113**, 081302 (2014), 1407.1052.
[25] N. Bozorgnia, G. B. Gelmini, and P. Gondolo, J. Cosmol. Astropart. Phys., **2010**, 019 (2010).
[26] S. Chang, G. D. Kribs, D. Tucker-Smith, and N. Weiner, Phys. Rev. D, **79**, 043513 (2009).
[27] D. Nygren, (2011), arXiv:1102.0815 [astro-ph.IM].
[28] R. Bernabei *et al.* (DAMA collaboration), Eur. Phys. J. C, **74**, 3196 (2014), arXiv:1409.3516 [hep-ph].
[29] E. Fernandez-Martinez and R. Mahbubani, JCAP, **1207**, 029 (2012), arXiv:1204.5180 [astro-ph.HE].
[30] J. Klinger and V. A. Kudryavtsev, Phys. Rev. Lett., **114**, 151301 (2015), arXiv:1503.07225 [hep-ph].
[31] V. A. Kudryavtsev, M. Robinson, and N. J. C. Spooner, Astropart. Phys., **33**, 91 (2010), arXiv:0912.2983 [hep-ex].
[32] J. I. Collar, Phys. Rev. C, **88**, 035806 (2013).
[33] E. Aprile *et al.* (XENON100), Phys. Rev. D, **84**, 061101 (2011).
[34] Z. Ahmed *et al.* (CDMS), Phys. Rev. D, **83**, 112002 (2011).
[35] J. Cherwinka *et al.* (DM-Ice), Phys. Rev. D, **93**, 042001 (2016).
[36] J. Cherwinka *et al.*, Astropart. Phys., **35**, 749 (2012).
[37] J. Cherwinka *et al.* (DM-Ice), Phys. Rev. D, **90**, 092005 (2014), arXiv:1401.4804 [astro-ph.IM].
[38] B. Ahmed *et al.* (NAIAD), Astropart. Phys., **19**, 691 (2003), arXiv:hep-ex/0301039 [hep-ex].
[39] A. Achterberg *et al.* (IceCube), Astropart. Phys., **26**, 155 (2006), arXiv:astro-ph/0604450 [astro-ph].
[40] D. Abriola *et al.*, Astropart. Phys., **20**, 133 (1999), ISSN 0927-6505.
[41] D. Engelkemeir, Rev. Sci. Instrum., **27**, 589 (1956).
[42] I. Khodyuk, P. Rodnyi, and P. Dorenbos, J. Appl. Phys., **107**, 113513 (2010), arXiv:1102.3799 [physics.ins-det].
[43] W. C. Pettus (DM-Ice), in *12th Conference on the Intersections of Particle and Nuclear Physics (CIPANP 2015) Vail, Colorado, USA, May 19-24, 2015* (2015) arXiv:1510.00378 [physics.ins-det].
[44] R. Bernabei *et al.* (DAMA), Nucl. Instrum. Methods Phys. Res., Sect. A, **592**, 297 (2008), arXiv:0804.2738

[astro-ph].
[45] J. Amaré *et al.* (ANAIS), Opt. Mater., **36**, 1408 (2014), arXiv:1401.3118 [physics.optics].
[46] K. Kim *et al.* (KIMS), Astropart. Phys., **62**, 249 (2015), arXiv:1407.1586 [astro-ph.IM].
[47] J. Amaré *et al.* (ANAIS), Nucl. Instrum. Methods Phys. Res., Sect. A, **742**, 187 (2014), arXiv:1308.3478 [physics.ins-det].
[48] S. Cebrián *et al.* (ANAIS), Astropart. Phys., **37**, 60 (2012), ISSN 0927-6505.
[49] Z. Pierpoint, Ph.D. thesis, University of Wisconsin (2016).